The Young Adult Human Brain: An MRI-based Morphometric Analysis

Pauline A. Filipek,[1] Christian Richelme,[1] David N. Kennedy,[1,2] and Verne S. Caviness, Jr.[1]

[1] Pediatric Neurology and [2] Radiology Services, Center for Morphometric Analysis, Massachusetts General Hospital, Harvard Medical School, Boston, Massachusetts 02129

Morphometric analysis was performed on three-dimensional MRI scans of 10 male and 10 female young adults with four principal objectives: (1) to characterize *in vivo* volumes of whole brain and substructures, (2) to explore volumetric symmetry in bilateral structures, (3) to consider the extent to which volumetric measures are dimorphic in the male and female brain, and (4) to provide a normal volumetric database for the young adult brain. Total brain volumes ranged between 1173 and 1626 cm^3. All bilateral structures were symmetric or nearly symmetric in volume, with the exception of a slightly larger right neocortex and amygdala, and larger left lateral ventricle. Male brains were larger in volume than female brains, a difference that reached significance for cerebellar but not for cerebral hemisphere volume. In females, there was less cerebral white matter while caudate volume was larger than in the male brains. The proportions of caudate and hippocampus relative to total cerebral volumes were larger in females than in males. These four measures accurately predicted gender in 85% of the subjects by discriminant analysis. No gender differences were noted in the structural symmetry analysis. These results represent the first step in establishing a comprehensive database of morphometric parameters, with unexpected findings relative to brain symmetry and sexual dimorphism.

Brain size is a useful general descriptor of ontogenetic process and outcome (Caviness et al., 1989; Filipek et al., 1992). Despite its potential contribution to studies of the normal and diseased brain, the parameter of size has had an ambiguous status in brain science. In part, this is the legacy of misuses of the parameter in the service of other than scientific agenda (Gould, 1981). Brain size has been a difficult parameter with which to work. In postmortem analyses, large and marginally predictable variability in the size of the brain or its anatomic components is inevitable, resulting from the sequence of processes spanning death and tissue preparation. Additionally, methods applicable to neuropathologic tissue are so tedious and time consuming that adequate sample sizes are seldom achieved (Filipek et al., 1989).

Some of the obstacles to the application of the parameter of size to brain science have been resolved by *in vivo* magnetic resonance imaging (MRI) and computer-assisted algorithms for morphometric analyses. This general methodology is applied here to the brains of 10 male and 10 female young adult volunteers to characterize the volumes of whole brain and substructures in this cohort, with particular analyses of structural asymmetry and gender effects. It is well recognized that there is distinctive asymmetry of cerebral surface topography (e.g., Bear et al., 1986) and even of individual cytoarchitectonic fields (e.g., Galaburda et al., 1978; Rademacher et al., 1993). The present investigation was undertaken to evaluate whether these recognized cortical asymmetries are associated with volumetric asymmetries of cerebral structures.

It has been reported that the female brain is approximately 10% smaller than the male brain (Zatz et al., 1982; Swaab and Hofman, 1984). In addition, sexual dimorphism has been reported in measures of sylvian fissure and corpus callosum in the human brain (Risse et al., 1989; Witelson, 1989; Kimura, 1992; Steinmetz et al., 1992; Witelson and Kigar, 1992); these findings potentially reflect gender differences in hemispheric laterality rather than in absolute volume measures (Swaab and Hofman, 1984). We undertook this analysis, therefore, with the expectation that the female brain would be found to be smaller than that of the male. However, lacking an a priori precedent, we anticipated that the general proportionality of the male and female brains would predict the proportionality of the component structures.

Cerebral Cortex July/Aug 1994;4 344–360; 1047-3211/94/$4.00

The results of these analyses provide unexpected findings relating to volumetric proportions of brain structures, volumetric symmetry, and sexual dimorphism in the young adult brain. The requisite imaging technology is widely available, as are various morphometric algorithms. These measures initiate a database that may be shared and expanded by other investigators and clinical laboratories concerned with human brain science and human brain disorders.

Materials and Methods

Subjects

MRI scans were performed with informed consent on 10 male and 10 female young adult volunteers. These 20 subjects include seven volunteers reported previously (Filipek et al., 1989). The mean age of the male subjects was 27.4 ± 5.0 years (19–37 years), while that of the female subjects was 26.9 ± 5.3 years (17–33 years). Seven males and eight females were strongly right-handed (≥6/7 items) using a modified handedness questionnaire (Oldfield, 1971); the remaining subjects were considered to be non-right-handed. The mean Hollingshead (1975) socioeconomic level for the male subjects' families was 54.1 ± 14.4 and for the female subjects was 56.2 ± 7.5. Nine males and 10 females were enrolled in college or had attained at least a bachelor's degree at the time of study; one male has an associate's degree. Seven males and seven females hold graduate degrees

MRI Image Acquisition

Coronal three-dimensional T_1-weighted spoiled gradient echo MRI scans were performed on two different imaging systems Ten FLASH scans on four males and six females were performed on a 1.5 tesla Siemens Magnetom MR System (Iselin, NJ) with the following parameters: TR = 40 msec, TE = 8 msec, flip angle = 50°, field of view = 30 cm, slice thickness = contiguous 3.1 mm, matrix = 256 × 256, and averages = 1 (Filipek et al., 1989). Ten 3D-CAPRY scans on six males and four females were performed on a 1.5 tesla General Electric Signa MR System (Milwaukee, WI), with the following parameters: TR = 50 msec, TE = 9 msec, flip angle = 50°, field of view = 24 cm, slice thickness = contiguous 3.0 mm, matrix = 256 × 256, and averages = 1. The MR image data sets were transferred by magnetic tape to our site for morphometric analyses.

Morphometric Analyses

Positional Normalization

The image data sets were processed on Sun Microsystems, Inc. (Mountainview, CA) computer workstations. A three-dimensional cartesian coordinate system, referenced to the decussations of the anterior (AC) and posterior (PC) commissures, and bisecting the interhemispheric fissure at the level of the PC in the coronal plane, was imposed upon each imaged brain (Talairach and Tournoux, 1988; Filipek et al., 1991a). The axes of this coordinate system are defined as follows: x-axis increasing laterally from the subject's right to left, y-axis increasing from posterior to anterior, and z-axis increasing from superior to inferior. Each native MRI scan was then reformatted by a homogeneous (nondeformation) transformation between the coordinates in each native MR image data set and the normalized presentation of that data set, consisting of three-dimensional translation and rotation. This transformation was imposed such that the AC-PC line is oriented along the y-axis, the mid-sagittal plane is in the y, z-plane, and the x-axis is, by definition, normal to the mid-sagittal plane (xy = transaxial, xz = coronal, and yz = sagittal orientations) (Talairach and Tournoux, 1988). The MR image data set was resliced into normalized 3.0 mm coronal and 1.0 mm sagittal scans for subsequent segmentation (Filipek et al., 1991a). This procedure eliminates the need for uniformity of head position at the time of imaging.

Image Segmentation

On each planar MR image, anatomic segmentation was performed using intensity contour mapping and differential intensity contour algorithms (Kennedy and Nelson, 1987; Filipek et al., 1989; Kennedy et al., 1989) on the positionally normalized T_1-weighted scan. In principle, the segmentation algorithms identify, classify, and create a continuous outline corresponding only to those voxel locations constituting the specified anatomic borders at image intensity transitions. This procedure does not rely on absolute signal intensity values, which is the premise of most global intensity thresholding techniques. Rather, it interpolates across signal intensity transition zones and assigns the pixels with intensity values closest to the contour value to constitute the border (Kennedy et al., 1989). Once the external borders of the hemispheres and ventricles have been extracted and saved on a given slice, a histogram of the signal intensity distribution for each hemisphere is used. Signal intensity characteristics of gray and white matter result in a bimodal distribution, the nadir of which defines the gray–white border (Kennedy et al., 1989) Each voxel is assigned, in its entirety, to the tissue class its signal intensity most closely matches. Voxels that actually contain both gray and white matter will have an intensity that is most similar to the tissue class occupying the majority of the voxel volume. To first approximation, the amount of white matter contained in voxels labeled as gray matter will be equivalent to the amount of gray matter included in voxels labeled as white matter. This approach decreases the error involved with visual choice of a border location, as well as error from some of the effects of volume averaging across the border. Further details on these operations have been described elsewhere (Kennedy, 1986; Kennedy and Nelson, 1987; Caviness et al., 1989; Filipek et al., 1989, 1991a, 1992; Kennedy et al., 1989). All primary image segmentation for this analysis was performed in the normalized coronal plane.

Anatomic Definitions

Anatomic structures may be defined by "primary" borders, corresponding to signal intensity transitions at brain–cerebrospinal fluid or at gray–white matter interfaces; "secondary" borders, knowledge-based anatomic subdivisions within a gray or white matter field that are not defined unambiguously by signal intensity transitions, must be subsequently defined by hand or algorithm by the investigator. Using primary and secondary borders, cerebral cortex and white matter, ventricular system, basal ganglia, mesencephalon and diencephalon, hippocampus, amygdala, brainstem and cerebellum were segmented for this analysis.

The following criteria were used for placement of the primary and secondary borders for the segmented structures (Fig. 1)

Cerebral hemispheres were divided at the midline in the coronal plane by a hand-drawn line connecting the measured midpoint of the corpus callosum with the midpoint of the hypothalamus, third ventricle, cerebral aquaduct, and so on. *Cerebral cortex* was defined medially by the cortico-white matter interface, and otherwise by the cortico-cerebrospinal (CSF) interface; *white matter* was defined by the gray matter–white matter interfaces; *ventricular system* (lateral ventricles, including frontal, temporal, and occipital horns in continuum; third and fourth ventricle) was defined by the ventricular–parenchymal interfaces; *caudate* (in continuum. head, body, tail superior to ventricular trigone, and ventral striatum) was defined superomedially by the interface with the lateral ventricles, inferiorly by the interface with the adjacent rostral peduncle of the thalamus when present, and otherwise by the interface with the adjacent white matter; *putamen* was defined medially by the external medullary lamina of the globus pallidus, laterally by the external capsule, and otherwise by adjacent white matter; *globus pallidus* (I and II) was defined superomedially by the interface with the internal capsule, inferiorly by the anterior commissure, ansa lenticularis, or nucleus basalis, when present, and laterally by the external medullary lamina; *central gray nuclei* (thalamus, pulvinar, hypo-, epi-, and subthalamus, substantia nigra, red nucleus, medial and lateral geniculate bodies) were defined superiorly by the interface with the rostral peduncle of the thalamus or body of the lateral ventricle, inferiorly by either the diencephalic–CSF interface or the secondary border defined below, and laterally by the internal capsule.

The *amygdala* (including nucleus basalis) and *hippocampus* (including alveus, uncus, dentate, subiculum, and retrosplenial gyri, but not parahippocampal gyri) were defined as a continuous volume *Amygdala* was defined superiorly by the interface with the ansa peduncularis, medially by the CSF interface, inferolaterally by white matter, and inferomedially by a secondary border connecting the medial tip of the subjacent white matter with the uncal notch; *hippocampus* was defined superolaterally by the interface with the inferior horn of the lateral ventricle, inferolaterally by white matter, and inferomedially by a secondary border connecting the medial tip of the subjacent white matter with the subiculum–parahippocampal gyrus interface. Following Talairach and Tournoux (1988), the secondary ventromedial transition from the *amygdala* anteriorly to the *hippocampus* posteriorly (Fig. 2) was subsequently calculated as occurring at 10/24 of the distance between the AC and PC for each brain.

The transition between the *central nuclear gray mass* and the *brainstem* was defined as a plane established by a secondary line drawn on a reconstructed 1 mm midline sagittal slice connecting the posterior commissure and the most inferior point of the interpeduncular fossa (Fig. 3). The inferior brainstem–cervical border was defined in the same midline plane by a line perpendicular to the axis of the brainstem 1 mm inferior to the obex of the fourth ventricle (Fig. 3) These superior and inferior borders were transformed into the coronal plane for segmentation (Kennedy et al , 1991); the lateral borders of the brainstem were subsequently defined in the coronal plane by a secondary vertical line connecting the inferiormost interface between CSF and the lateral lemniscus with the glossopharyngeal nerve.

The total *cerebellum* was divided by a secondary border connecting the midline of the central lobule and uvula, excluding the fourth ventricle. *Cerebellar cortex* was defined at the cerebellar–CSF interfaces, white matter interface, or secondary brainstem border; *cerebellar central mass* (including the middle cerebellar peduncle) was defined by the interface with cerebellar cortex and secondary brainstem border, to include central gray matter structures, which were not felt to be reliably distinguished from the cerebellar white matter

Volumetric Analysis

The total number of voxels for each structure was multiplied by the absolute volume of each voxel (Kennedy and Nelson, 1987; Kennedy et al , 1989), which was determined by the imaging parameters.

Data Analysis

All statistical computations were performed by SAS statistical analysis software (SAS Institute Inc., Cary, NC) Between-group comparisons for age, scanner system, and gender effects were performed using a multivariate approach to repeated-measures analysis of variance (MANOVA) (Maxwell and Delaney, 1990). Comparisons of left–right volumetric symmetry were based upon a symmetry coefficient (Galaburda et al., 1987), $(L - R)/[0.5(L + R)]$, followed by the Student's t test to assess the probability that the mean of the distribution of symmetry coefficients was nonzero. Correlations between left and right structures were performed using the Pearson product-moment correlation coefficient and significance probability. To control type I errors, the Bonferroni adjustment was used to maintain α at 0.05 for the univariate symmetry coefficients and Pearson correlations

A linear discriminant analysis was performed to

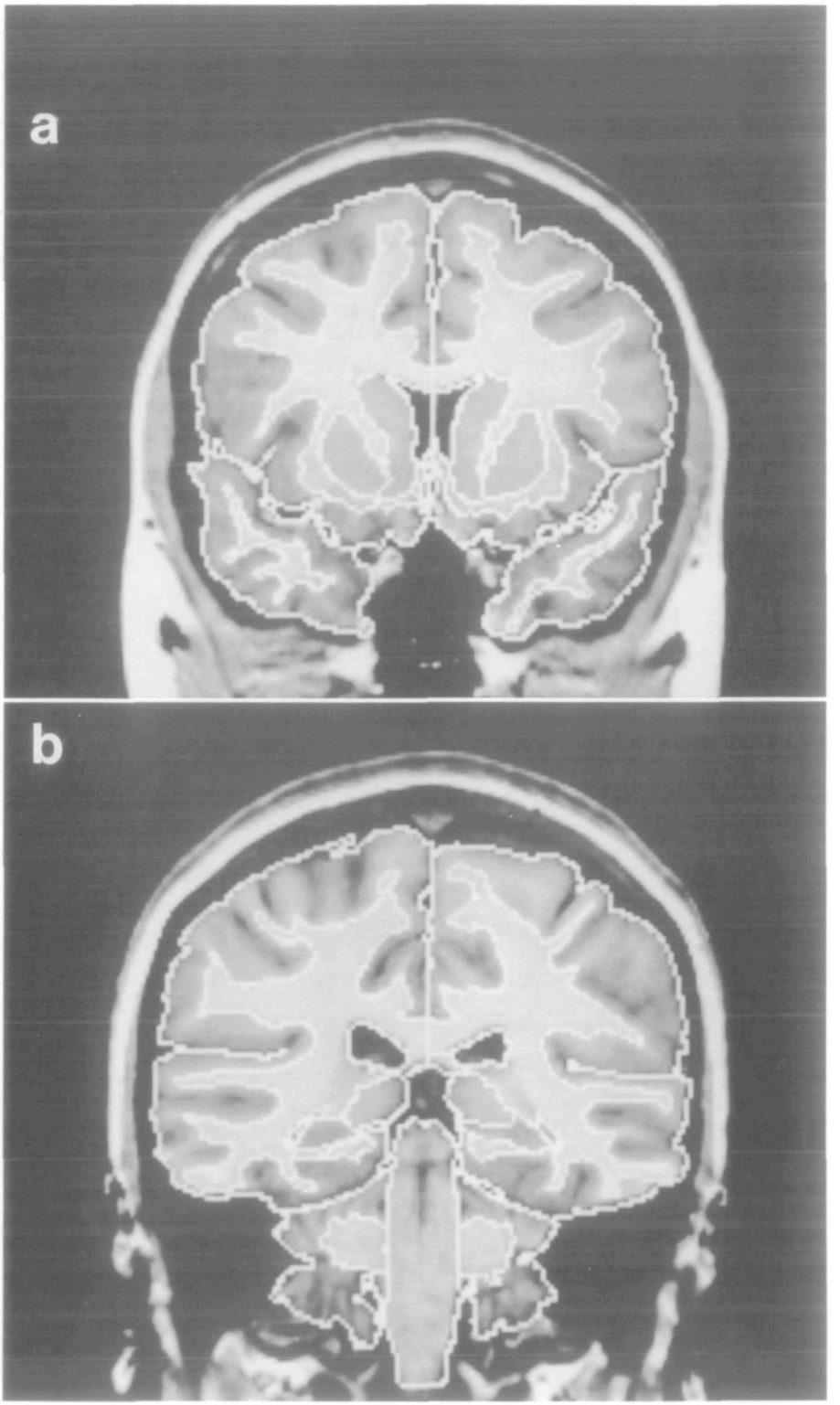

Figure 1. Anterior (*top*) and posterior (*bottom*) representative coronal slices demonstrating the resulting segmentation outlines.

determine the extent to which the significant dimorphic measures are predictive of gender of each subject. A cross-validation method classified each subject in turn, using a discriminant function derived from the other 19 subjects. The resulting number of correct and incorrect classifications is reported. The morphometric correlations with handedness in this population will be considered in a subsequent analysis that will incorporate measures of the area of the corpus callosum.

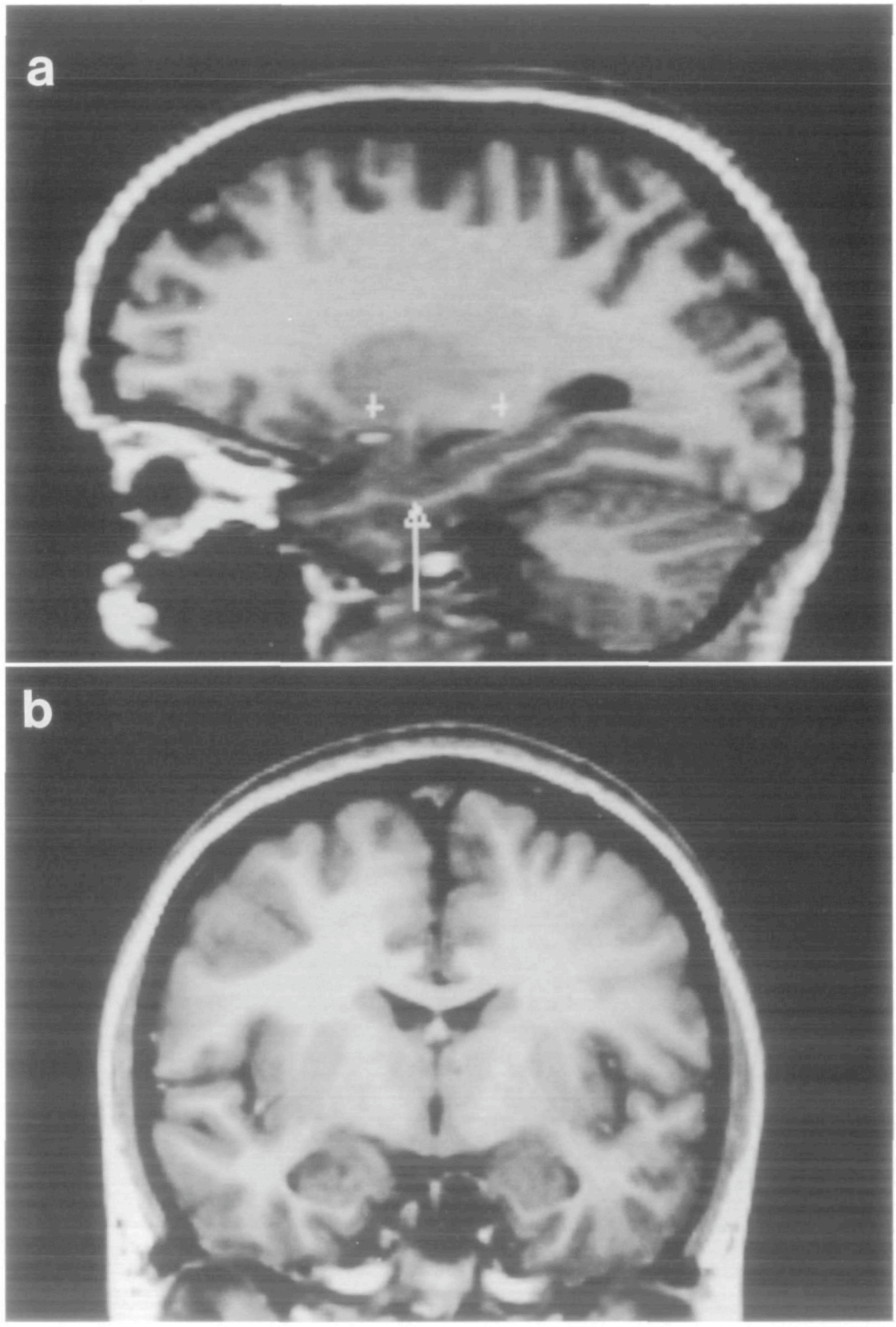

Figure 2. Anatomic definition of the transition between amygdala and hippocampus. *a*, Sagittal slice showing the transition point at 10/24 of the distance between the anterior and posterior commissures. *b–d*, Coronal slices at the transition (*b*), and adjacent anterior (*c*) and posterior (*d*) slices.

Results

Subject Variability

There were no significant differences in age or socioeconomic factor between the male and female adults No significant effects on any of the measured volumes of ventricles, gray or white matter structures were found to result from the use of the two different MRI manufacturers in this analysis (Siemens FLASH vs General Electric 3D-CAPRY) or from the unequal distribution of males and females imaged by each scanner system ($p > 0.35$). There were also no differences

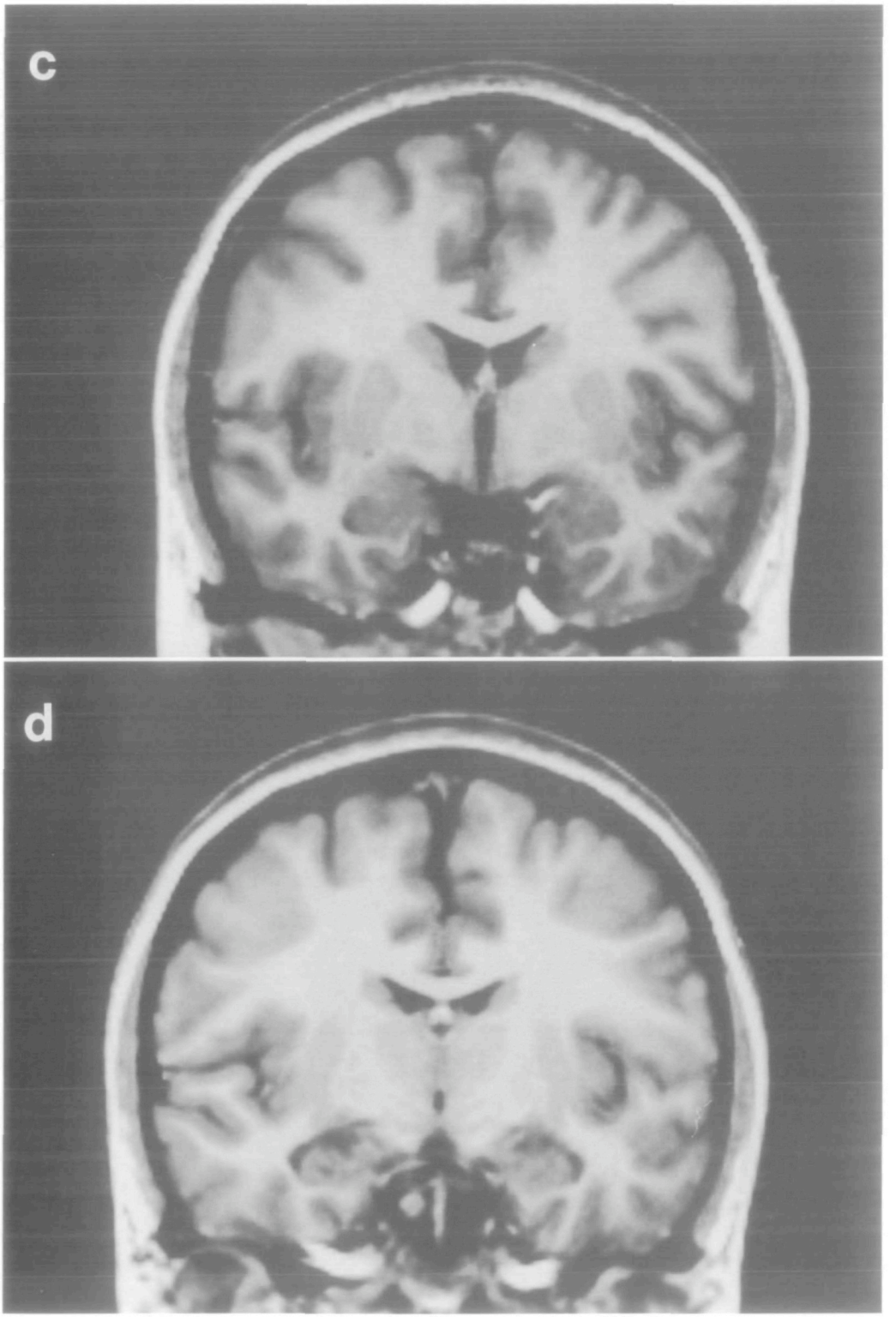

Figure 2. Continued.

in age between the male and female subjects scanned by the two scanner systems ($p > 0.53$).

Volume Measures

The total volume of the young adult brains in this series lies in the range of 1173.33–1625.62 cc^3 (Table 1). The cerebrum is nearly 90% of total brain volume, eight times the volume of the cerebellum and over 50 times that of the brainstem or total ventricular system.

Gray matter structures contribute over 60% of total cerebral volume (Fig. 4). The neocortex is the dominant gray matter structure of the cerebrum, contributing 58% of total cerebral volume and 92% of total

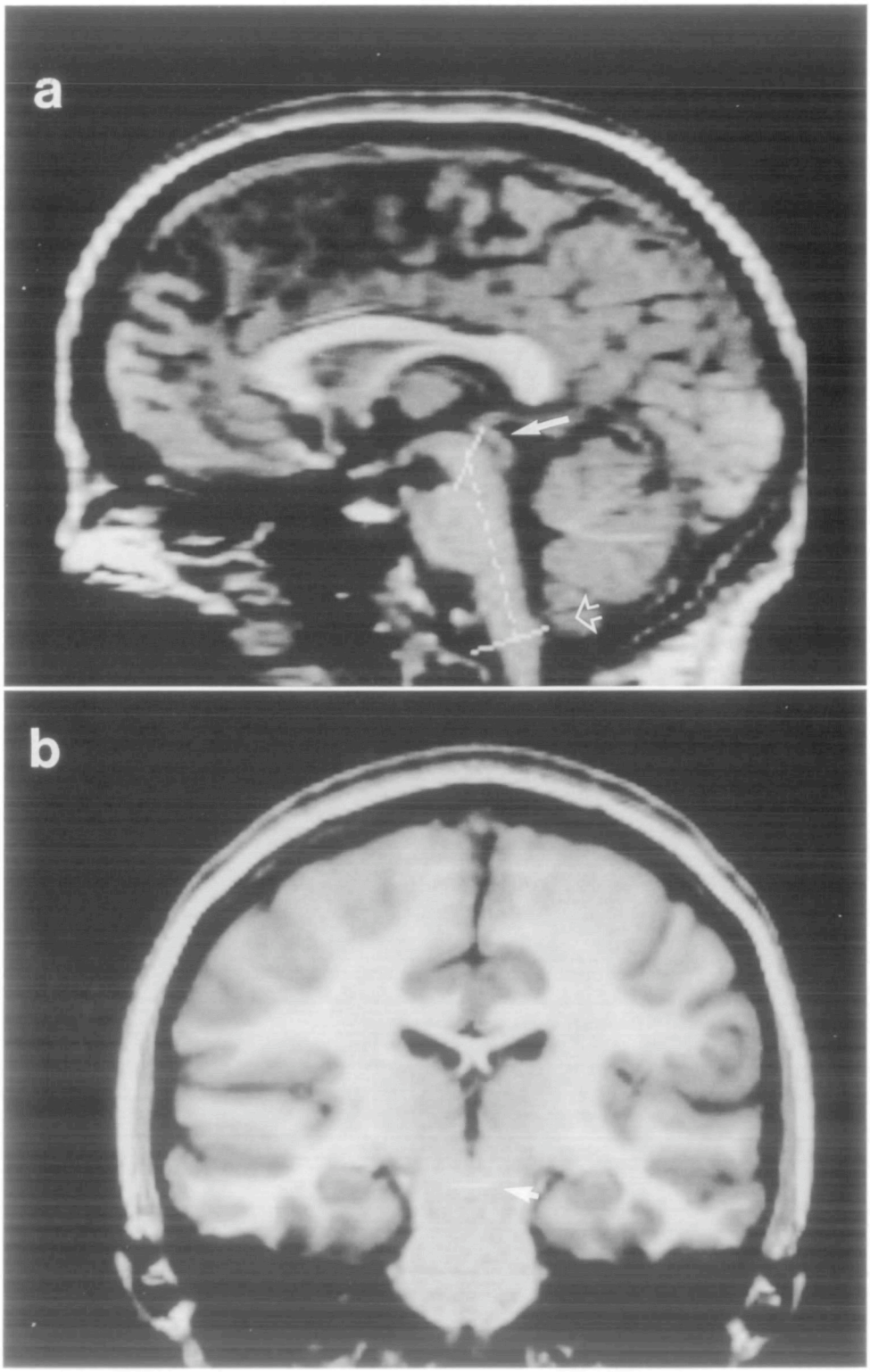

Figure 3. *a*, Midsagittal slice demonstrating the brainstem–diencephalic border (*solid arrow*) and the brainstem–cervical border (*open arrow*), which are transformed onto the coronal plane for segmentation. *b* and *c*, Coronal planes showing the resulting superior and inferior borders (*arrows*) after the transformation.

gray matter volume. The volume of the cerebral white matter, composed principally of myelinated axons mediating neocortical connectivity, is 37% of total cerebral hemisphere. The ratio of cerebral white matter to neocortical volume is 0.64.

In contrast to the prominence of the neocortex, each of the separate subcortical gray matter structures of the cerebrum contributes only 0.5–1.7% of the total cerebral volume (Fig. 4). The ratios of neocortical volume to the volumes of the principal forebrain gray matter structures are therefore large (Fig. 5). These range from approximately 34:1 for the neocortical-to-

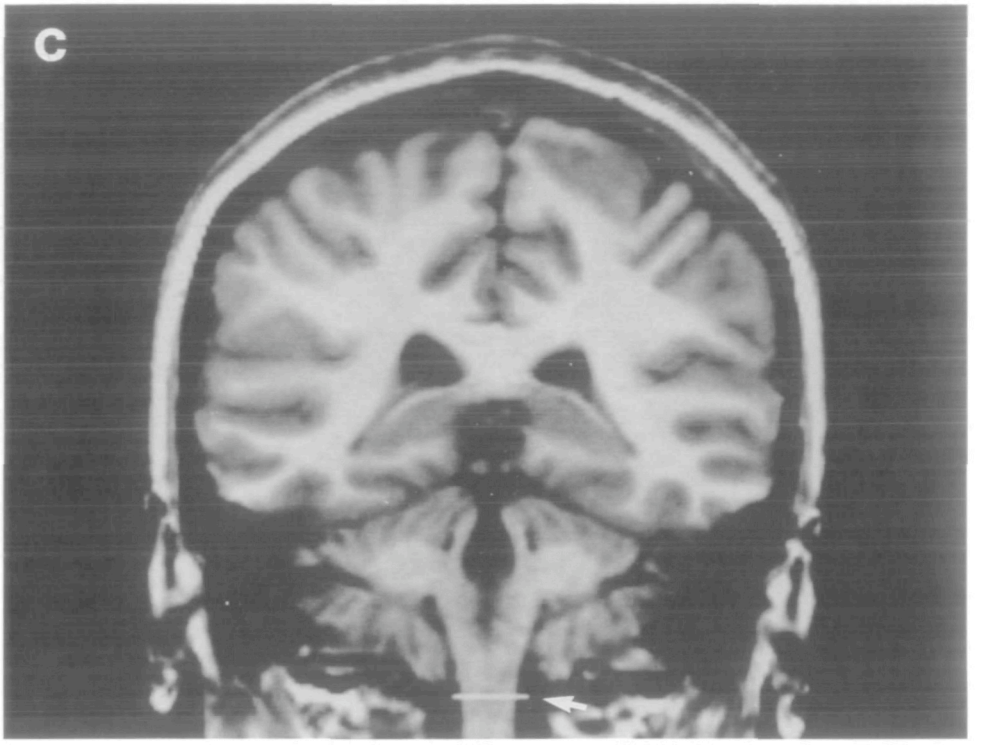

Figure 3. Continued.

diencephalic volumetric ratio, to 127:1 for the neocortical-to-amygdala ratio. The ratios of neocortical volume to the volumes of hippocampus and caudate nucleus are similar at approximately 70:1, and the ratio to the volume of the lenticular nucleus is approximately 50:1.

The volumes of the individual forebrain nuclear structures differ much less from each other (Table 1). Thus, the volumes of the central gray nuclei and the striatum (the sum of caudate and putamen nuclei) are similar, as are the volumes of the caudate and putamen. The putamen is 2.5 times larger than the pallidum, while the hippocampus is nearly twice the volume of the amygdala.

The coefficients of variability (CV) for volumes of structures other than the lateral ventricles range from

Table 1
Volumes of principal brain structures in cc^3, combined male/female, right/left ($N = 20$)

Structure	Mean ± SD	CV (%)	Min	Max	% Total
Whole brain	1380.1 ± 113.9	8.3	1173.3	1625.6	100.0
Total cerebrum	1192.1 ± 102.5	8 6	1007.5	1403.5	86.4*
Neocortex	688.8 ± 65.0	9.4	573.7	8?8.5	57.8
White matter	443.8 ± 42.4	9.6	376.2	51?.?	37.2
Caudate	9.5 ± 1.3	13.8	7.3	11.7	0 8
Lenticulate	14.1 ± 1.1	8.6	11 9	16 6	1.2
Putamen	10.1 ± 0.9	8.4	8.7	1.4	0.9
Pallidum	3.9 ± 0.5	12.6	3.1	5.2	0.3
Hippocampus	9.9 ± 1.2	12.4	7.2	11.5	0.8
Amygdala	5.5 ± 0.8	13.9	4.0	7.0	0.5
Central gray nuclei	20.5 ± 1.7	8.3	18 1	24 1	1.7
Total cerebellum	143.4 ± 12.5	8.7	123.8	175.1	10.4*
Cortex	119.7 ± 10.6	8.8	102.9	146.3	83.5
Central mass	23.7 ± 2.9	12.5	19 1	29.6	16.5
Ventricular system	21.3 ± 7.4	34.7	10.3	36.4	1.5*
Lateral	18.1 ± 7.3	39.9	7.3	33.7	85.0
Third	1.3 ± 0.5	36.9	0.3	2.2	6.1
Fourth	1.9 ± 0.6	32.4	1 0	3.6	8.9
Brainstem	23.4 ± 3.1	13.1	19.5	32.3	1.7*

* Percentage of total expressed as proportion of whole brain volume. Other substructures are expressed as proportion of total cerebrum, cerebellum, or ventricular system, respectively.

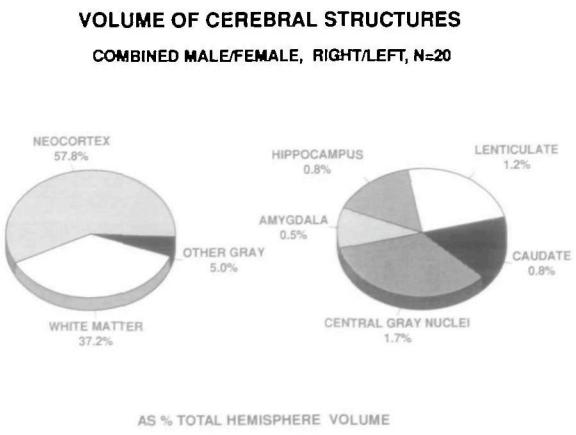

Figure 4. Proportionate volumes of cerebral structures.

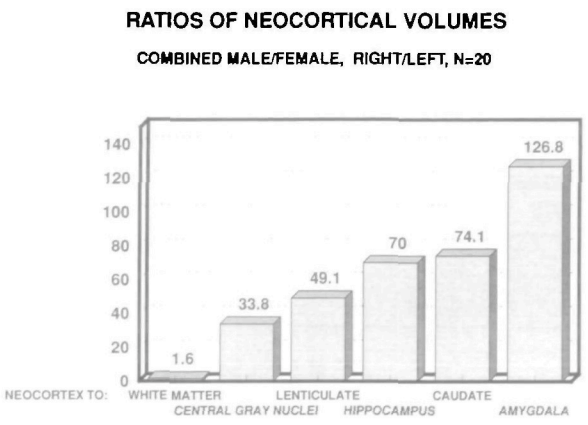

Figure 5. Graphic representation of neocortical mean volume ratios.

8% to 14%. The volumes measured for the lateral ventricles range from 7 to 34 cc^3, with a CV of 40%.

Comparison of Bilateral Brain Structures

Bilateral structures of the cerebrum and cerebellum, with the exceptions specified in the following paragraph, were not detectably asymmetric in volume. The Pearson product-moment correlation coefficients were 0.9 or greater ($p < 0.0001$) for the right versus left volumes of the total cerebrum, neocortex, cerebral white matter, caudate, and cerebellum. Coefficients were greater than 0.6 for the estimated volumes of the remaining structures (Table 2).

Significant asymmetries of relatively small magnitude were noted between only three forebrain structures (Fig. 6). The neocortex of the right hemisphere averaged 3.7 cc^3 larger than the left, but this asymmetry was consistent across the cohort ($p < 0.004$); the white matter measures were symmetric. Other significant asymmetries included a 9% larger right amygdala ($p < 0.002$), and 18% larger left lateral ventricle ($p < 0.01$). The mean volume of the right cerebral hemisphere tended to be slightly larger than the left, while the left hippocampus and left caudate tended to be larger than the right, but these differences were not significant in this cohort ($p > 0.06$). It should be noted that the relatively small sample size may limit the sensitivity of the analyses to true symmetry differences in the smaller structures.

Gender Effects

The male whole brain volume was 8% larger than the female volume ($p < 0.02$; Table 3, Fig. 7, top). The male cerebrum was 7% larger than that of the female, although this difference did not reach significance ($p < 0.06$). Among the structures of the cerebral hemispheres, only two were noted to demonstrate gender differences in these subjects (Fig. 7, bottom). The volume of the white matter was 8% less in female than male brains ($p < 0.05$), while the caudate nuclei were 12% larger in the female brains ($p < 0.03$).

The male cerebellum was 11% larger than that of the female ($p < 0.002$). Of note is the difference between the volumes of male and female cerebellar central mass ($p < 0.05$), which was of less magnitude than the differences between the cerebellar cortical measures ($p < 0.0003$)

In contrast to the gender differences noted for the absolute volumes, there were no differences noted between males and females for the following volumetric proportions (Table 4, Fig. 8): cerebrum, cerebellum, and brainstem relative to whole brain, or cerebellar cortex and central mass relative to total cerebellum. Only the volumetric proportions of caudate ($p < 0.001$) and hippocampus ($p < 0.02$) relative

Table 2
Comparison of bilateral brain structures, combined male/female ($N = 20$)

Structure	Right (mean ± SD)	Left (mean ± SD)	Symmetry coefficient	$p <$	Pearson coefficient	$p <$
Total cerebrum	606.3 ± 53.5	603.9 ± 54.1	−0.0039	NS	0.991	0.0001
Neocortex	346.2 ± 33.0	342.6 ± 32.2	−0.0104	0.004	0.988	0.0001
White matter	221.8 ± 20.7	221.1 ± 22.2	−0.0036	NS	0.968	0.0001
Caudate	4.7 ± 0.7	4.8 ± 0.7	0.0244	NS	0.900	0.0001
Putamen	5.1 ± 0.4	5.0 ± 0.5	−0.0184	NS	0.744	0.0002
Pallidum	1.9 ± 0.3	1.9 ± 0.3	0.0275	NS	0.616	0.004
Central gray nuclei	10.2 ± 0.9	10.3 ± 0.9	0.0095	NS	0.850	0.0001
Amygdala	2.9 ± 0.4	2.6 ± 0.4	−0.0967	0.002	0.749	0.0001
Hippocampus	4.9 ± 0.7	5.1 ± 0.7	0.0396	NS	0.732	0.0002
Lateral ventricles	8.1 ± 3.1	9.9 ± 4.6	0.1820	0.01	0.754	0.0001
Cerebellum	71.5 ± 6.4	71.9 ± 6.1	0.0047	NS	0.961	0.0001

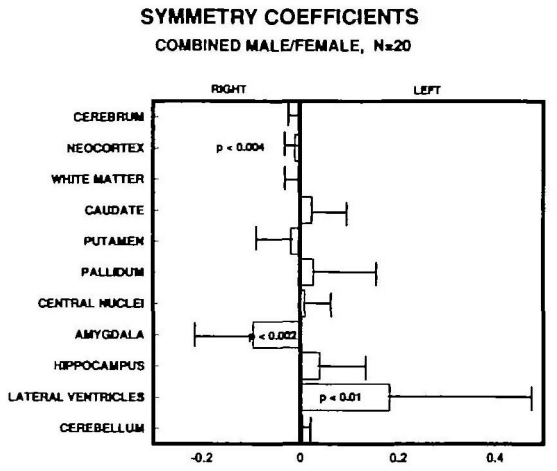

Figure 6. Graphic representation of symmetry coefficients The error bars represent 1 standard deviation from the mean

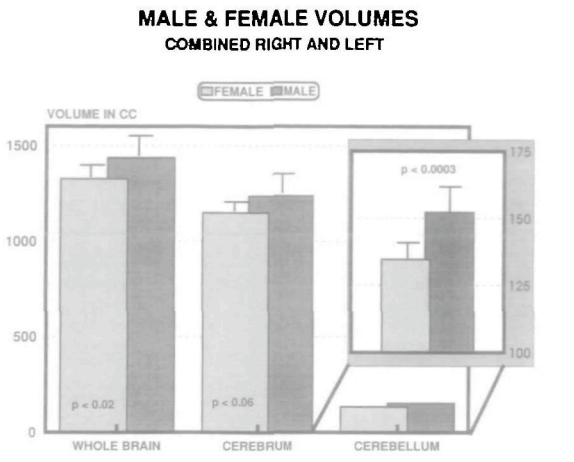

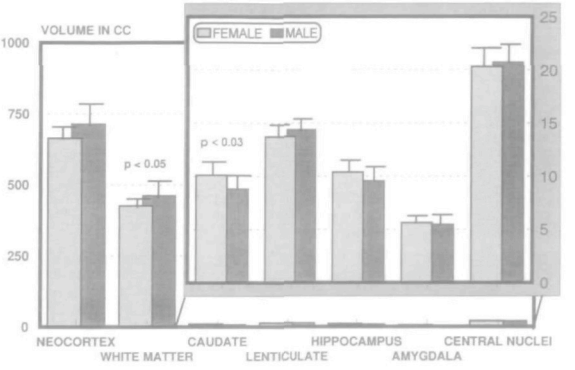

Figure 7. Graphic representation of male and female whole brain (A) and structural (B) mean volume differences. The error bars represent 1 standard deviation from the mean

to total cerebrum differed between the sexes, with a larger proportion found for these structures in the female brain None of the other cerebral volumetric proportions were found to be dimorphic, including the white matter. Thus, the proportions of the major brain regions, most cerebral and all cerebellar substructures were similar in male and female brains, with the exception of the caudate and hippocampus.

Discriminant analysis on total cerebellar volume resulted in a correct classification of 19 of the 20 subjects, with one male misclassified. Analysis on absolute caudate and white matter volumes, and on proportions of caudate and hippocampus both resulted in correct classification of 17 of the 20 subjects. The same three subjects (one female and two males) were misclassified by the latter two analyses, but not the

Table 3
Male and female structural volumes in cc^3, right/left combined

Structure	Male (mean ± SD, $N = 10$)	Female (mean ± SD, $N = 10$)
Whole brain*	1434.8 ± 116.2	1325.4 ± 85 4
Total cerebrum**	1235.6 ± 109.6	1148.5 ± 77 2
Neocortex	714.4 ± 69.4	663.2 ± 51 5
White matter**	462.4 ± 46.2	425.3 ± 30.0
Caudate**	8.8 ± 1.2	10.1 ± 1.1
Lenticulate	14.4 ± 1.2	13.7 ± 1.1
Hippocampus	9.6 ± 1.4	10.4 ± 1.0
Amygdala	5.5 ± 0 7	5.6 ± 0.9
Central gray nuclei	20.7 ± 1.7	20.3 ± 1.8
Total cerebellum*	152.2 ± 10.5	134.6 ± 6.8
Cerebellar cortex***	127 2 ± 8.9	112.3 ± 5.9
Central mass***	24.9 ± 3.3	22 4 ± 2 0
Ventricular system	22.6 ± 7.6	20.0 ± 7.3
Lateral ventricles	18.9 ± 7.6	17.3 ± 7.2
III ventricle	1.5 ± 0 5	1.1 ± 0.4
IV ventricle	2.1 ± 0 7	1.7 ± 0.5
Brainstem	24.5 ± 3.4	22.3 ± 2.3

* MANOVA: whole brain subdivisions, $F = 5.36$, $p < 0.01$ ANOVA. whole brain total, $F = 5.76$, $p < 0.02$, cerebellum, $F = 19.60$, $p < 0.0003$.

** MANOVA: cerebral subdivisions, $F = 3.44$, $p < 0.03$. ANOVA: cerebrum total, $F = 3.95$, $p < 0.06$; caudate, $F = 5.91$, $p < 0.03$; white matter, $F = 4.54$, $p < 0.05$.

*** MANOVA: cerebellar subdivisions, $F = 9.47$, $p < 0.002$. ANOVA: cerebellum total, $F = 19.60$, $p < 0.0003$; cerebellar cortex, $F = 19.60$, $p < 0.0003$; cerebellar central mass, $F = 4.61$, $p < 0.05$.

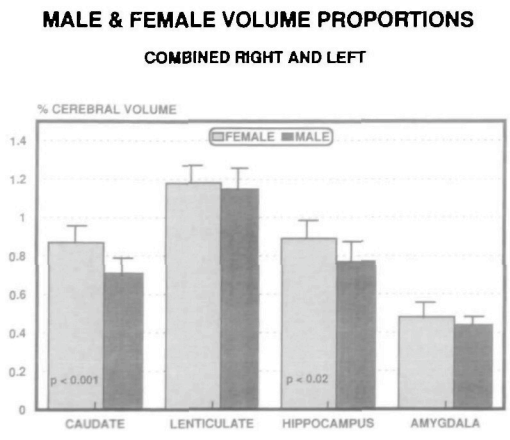

Figure 8. Graphic representation of male and female mean volume proportion differences for representative structures. The error bars represent 1 standard deviation from the mean.

male misclassified by the cerebellar discriminant analysis. The measures used for these gender classifications were preselected on the basis of their gender-group mean differences, and therefore these rates may not generalize to a new subject sample.

There were no differences noted between males and females in the symmetry or Pearson coefficients for left and right volumes of cerebrum, cerebellum, or component substructures.

Discussion

MRI-based morphometric analyses in these young male and female adult subjects noted total brain volumes ranging between 1173 and 1626 cm^3. Most substructures were symmetric in volume except for a larger right neocortex and amygdala, and larger left lateral ventricle. Male brains were larger in volume than female brains, a difference that reached significance for cerebellar but not for cerebral hemisphere volume. In females, there was less cerebral white matter while caudate volume was larger than in the male brains. The proportions of caudate and hippocampus relative to total cerebral volumes were larger in females than in males. These four measures accurately predicted gender in 85% of the subjects by discriminant analysis. No gender differences were noted in the structural symmetry analysis.

It remains to be established to what extent this series of 20 subjects is representative of a "normal population." This analysis provides, in any event, an orienting perspective with regard to the volumes of the young adult brain. These values were obtained at ages when brain volume should be maximum, as brain volume of "normal" individuals progressively declines beyond the fourth or fifth decade at a rate variously estimated to be from 1% to 3.5% per decade (Dekaban and Sadowsky, 1978; Miller et al., 1980; Harper and Mina, 1981; Hubbard and Anderson, 1981; Hatazawa et al., 1982).

A variety of measurements have been recorded in the neuropathological literature for the total volume of the brain (or volume estimated from weight), for the major regions of the brain, and for certain substructures such as the hippocampus. These have been obtained after various schedules of fixation or histological processing methods, some with estimated corrections for the degree of postprocessing shrinkage. In general, these measurements range from about 25% to 30% less to approximately the same as the volumes reported here (Wessely, 1970; Paul, 1971; Dekaban and Sadowsky, 1978; Kretschmann et al., 1979, 1986b; Holloway, 1980; Harper and Mina, 1981; Klekamp et al., 1987; Pakkenberg, 1988). These volumes are also in accord with those determined by similar morphometric methods in this laboratory but based upon a sample of only seven subjects (Filipek et al., 1989).

Although many other imaging studies have reported various morphometric measures based on MRI over the past decade, many of these were limited to linear measures on single slices, or area measurements on slices separated by a 2–3 mm gap. Therefore, comparison of the volumes reported here with other prior studies must consider comparable scanning and morphometric techniques, as well as comparable subject populations and anatomic definitions (Filipek et

Table 4
Male and female volumetric proportions, right/left combined, as percentage of total

Structure	Male (mean ± SD)	Female (mean ± SD)
Total cerebrum	86.1 ± 1.1[a]	86.6 ± 0.7[a]
Neocortex	56.9 ± 1.6	56.9 ± 1.4
White matter	36.9 ± 1.7	36.5 ± 1.2
Caudate[b]	0.7 ± 0.1	0.9 ± 0.1
Lenticulate	1.2 ± 0.1	1.2 ± 0.1
Hippocampus[b]	0.8 ± 0.1	0.9 ± 0.1
Amygdala	0.4 ± 0.1	0.5 ± 0.1
Central gray nuclei	1.7 ± 0.2	1.8 ± 0.2
Total cerebellum	10.7 ± 1.1[a]	10.2 ± 0.7[a]
Cerebellar cortex	83.6 ± 1.7	83.4 ± 1.2
Central mass	16.4 ± 1.7	16.6 ± 1.2
Lateral ventricles	1.5 ± 0.5[a]	1.5 ± 0.6[a]
Brainstem	1.7 ± 0.2[a]	1.7 ± 0.2[a]

[a] Percentage of total expressed as proportion of whole brain volume. Other substructures expressed as proportion of total cerebrum or cerebellum, respectively.

[b] MANOVA: cerebral subdivisions, $F = 3.03$, $p < 0.05$. ANOVA: caudate, $F = 15.45$, $p < 0.001$, hippocampus, $F = 7.22$, $p < 0.02$.

al., 1992). In general, our whole brain and cerebrum volumes are in accord with those of other investigators (DeLisi et al., 1991; Coffey et al., 1992; Harris et al., 1992). A conspicuous exception is with regard to our cerebellar volumes, which are over 20% larger than those reported by Escalona et al. (1991). These authors used substantially different methods involving systematic sampling and point counting for volume estimates Their definition for inclusion or exclusion of voxels only partially containing cerebellum is not stated; excluding partial voxels would directly result in underestimation of cerebellar volume. Also, their anatomic definition of the cerebellum is not clearly comparable with the one used here, which may further contribute to the volume differences.

The caudate volumes are in accord with Breier et al. (1992), whose anatomic definitions appear very similar to those used here, in contrast to those studies that measured only the head of the caudate (DeLisi et al., 1991; Harris et al., 1992). Other studies of putamen (Harris et al., 1992) and lenticulate (DeLisi et al., 1991) volumes are also concordant given somewhat differing imaging techniques.

The lateral ventricular volumes reported here differ from those previously reported in the literature, ranging from 25% to 45% larger; however, these latter ventricular volumes are still within 1 standard deviation (SD) of our mean volumes (DeLisi et al., 1991; Coffey et al., 1992; Shenton et al., 1992). The CV of the volumes in this study is 40%, while other studies report a CV of approximately 30% (DeLisi et al., 1991; Shenton et al., 1992). However, one study of normal adult volunteers, ranging in age from 30 to 91 years, has reported a CV of 70% for volumes of the lateral ventricles (Coffey et al., 1992). These differences probably reflect anatomic variation within the present subjects, rather than variability in measurement, as the borders between the ventricles and surrounding brain parenchyma are substantially less ambiguous than the borders defining other structures.

The absolute volumes for the amygdala and hippocampus reported here are 20% and 2% smaller, respectively, than those determined by MRI morphometry in a comparable, although smaller, group of young adults using similar imaging sequences (Watson et al , 1992). Although our exterior boundary criteria for these structures appear similar, our methods for this analysis differ in a significant regard. The rostral–caudal transition of amygdala to hippocampus can be difficult to define reliably, even using positionally normalized MRI scans. Therefore, an atlas-based (Talairach and Tournoux, 1988) algorithm-calculated secondary boundary was utilized, which may be the source of the differences. When the mean volumes for both structures are summed, the mean volumes of Watson et al. (1992) for "amygdala-hippocampus complex" are within 10% (1.1 SD) of our mean volumes.

Another study of amygdala and hippocampus volumes (Breier et al., 1992) followed somewhat similar exterior border definitions, but used the trigone of the lateral ventricles as the posterior border in the coronal plane (anterior to our posterior definitions). This analysis also did not include slices visualizing the amygdala–hippocampal transition, resulting in individual volumes that are 25–40% smaller than those reported here. However, their reported volume of the hippocampus–amygdala complex, which included the transition slices, is only 15% (1.7 SD) smaller than the present volumes, most likely reflecting the differing posterior borders.

In contrast, the hippocampal volumes reported here are approximately 45% larger than those reported by Jack et al. (1989) This discrepancy can be explained partially by the fact that the latter study defines the posterior borders of the hippocampus by a plane perpendicular to the sylvian fissure that intersects the posterior commissure, and that appears to be approximately 65° oblique to the AC-PC line. Application of this posterior plane to the hippocampal outlines produced in this study results in a 24% decrease from the mean hippocampal volume reported in Table 1, which nonetheless remains approximately 20% larger (1.7 SD). Much of this remaining difference can be due to the fact that the volumes reported by Jack et al. (1989) were normalized for intracranial volume and did not include the volume of the uncus. Differences in the MRI pulse sequence parameters (spin echo vs spoiled gradient echo) as well as in slice thickness (5 mm to 3 mm) between the latter and present studies may also be significant in this regard (Filipek et al., 1992).

Overall, it would seem that comparable morphometric measures are being obtained from many laboratories. Most of the discrepancy in reported volumes can be attributed to differing anatomic definitions, with additional contributions from differing imaging parameters. It is also highly probable that, despite varying anatomic definitions, the greatly improved anatomic resolution noted in the successive generations of MRI scanner software will further decrease these discrepancies in future studies.

Validation and Reliability of the Morphometric Method

Measurements in this laboratory, based upon phantom models, indicate that volumetric estimates based upon this MRI-based method of morphometry lie within 5–10% of the actual volumetric values, with average coefficients of variation less than 10% (Caviness et al., 1989; Filipek et al., 1989, 1992). These validation studies with phantoms have confirmed, as might be expected, that error and variation of measurement are inversely related to object size and MRI slice thickness. Error and variability of measure increase with surface irregularity and when the long axis of the imaged structure is parallel to the imaging plane, rather than perpendicular (Kennedy et al., 1989). Error and variation are further increased for objects less than 10 cc^3 in volume. These phantom studies also demonstrated that the coefficient of variability is minimized without an associated increase in measurement error by positional normalization of the imaged object prior to segmentation (Filipek et al., 1990).

The reliability of the method has been tested by repeated morphometric analyses of the same young adult brain, imaged seven times over several years on both imaging systems utilized for this study with segmentation performed by a single investigator. In this analysis of reliability, the coefficients of variation of the measures of the entire brain and the various substructures averaged less than 5% and did not exceed 8% (Filipek et al., 1991b). Interobserver reliability in the conduct of similar analyses elsewhere (Jack et al., 1990) has also been estimated at 93%

Bilateral Symmetry

The measured volumes of most bilaterally represented structures are symmetric. The significant exceptions are the larger right cerebral cortex, right amygdala, and left lateral ventricle. These observations based upon MRI morphometry confirms the observation of symmetry in postmortem specimens (Klekamp et al., 1987) and by computed tomographic-based morphometric analysis (Schwartz et al., 1985). Symmetry among a set of bilateral brain structures comparable to the set considered here has also been observed with the developing brains of *Macaca nemestrina* (DeVito et al., 1989).

In the analyses of Jack et al. (1989) and Watson et al. (1992), the right hippocampus was found to be approximately 10% greater in volume than the left hippocampus. In this study, analysis of symmetry did not demonstrate significant differences. When our hippocampal volumes were recalculated according to the definitions of Jack et al. (1989), the measures remained symmetric, as were those reported by Breier et al (1992). Watson et al. (1992) also reported slightly larger right amygdala volumes (3%). These discrepancies in amygdala and hippocampal asymmetry may be the result of the differing anatomic definitions used, in particular the anterior boundary of the hippocampus, as discussed above. Further analyses will be needed to reconcile these and other discrepancies that may emerge in the volumetric measurement of small structures by this general MRI-based methodology using the present anatomic definitions.

Volumetric symmetry of structures of the human brain is, perhaps, surprising given the characteristic asymmetry of cerebral surface topography. This is particularly apparent in the asymmetry of the frontal and posterior transverse diameters (LeMay and Kido, 1978; Bear et al., 1986; Kertesz et al., 1990) and the size, relative position, and configuration of sylvian (Geschwind and Levitsky, 1968; Steinmetz et al , 1989, 1990; Falk et al., 1991; Witelson and Kigar, 1992) and other fissures (Zilles et al., 1988; Ono et al., 1990; Bohm et al., 1991; Falk et al., 1991; Greitz et al., 1991, Rademacher et al., 1992). By implication, then, those developmental mechanisms that result in the symmetry of corresponding bilateral structures must not only be rigorously developmentally regulated, but must also act independently of the developmental mechanisms that govern the asymmetric shape and topographic details of the principal substructures. Indeed, Kertesz et al. (1990) have suggested that regional asymmetries, such as right frontal and left occipital petalias, might result from the effects of a three-dimensional "torque" on the two hemispheres during development.

The areas of certain neocortical cytoarchitectonic fields, for example, those of the posterior temporal plane, may be substantially asymmetric in the two hemispheres of the same individual (Galaburda et al., 1978; Jouandet et al., 1989; Rademacher et al., 1992) whereas the areas of other fields are typically concordant in the two hemispheres (Rademacher et al., 1992, 1993). The volume of the right temporal lobe (rostral to an oblique coronal plane passing through the posterior commissure) has been found to be approximately 15–20% greater than that of the left (Jack et al., 1988). The volumetric symmetry of total hemisphere and neocortex suggests that asymmetry of architectonic fields and individual lobes of the brain must be associated with compensatory variations in the size of other fields or lobes rather than with relative variation of the overall hemispheric or neocortical volumes in the two hemispheres. Such compensations might be limited to a small number of fields or to lobes proximate to each other, or they might be more generally distributed among fields or lobes of the entire neocortex.

Sexual Dimorphism

The measures undertaken here confirm the general experience, based upon postmortem specimens (Swaab and Hofman, 1984), or by inference from measures of head circumference (Jernigan and Tallal, 1990), or computed tomography (Zatz et al., 1982), that the volume of the adult normal female brain is approximately 10% less than the volume of the male brain. Whereas crude proportional allometric scaling does occur across species, it does not account for dimorphism within species in general and in the human brain in particular (Jerison, 1973). The disproportionate variation in the volumes of male and female brain regions and substructures reported here is not consistent with a simple allometric explanation for the sexual dimorphism.

In the present series, the lower volume of the female brain was found to be dominated by lower volumes of the cerebellum and of the cerebral white matter. The proportionate volumes of the cerebellum with respect to the entire brain and the cerebral white matter with respect to the cerebrum did not differ in male and female brains. The caudate nucleus, by contrast, was not only larger in absolute volume in the female brain but the proportionate volume of this structure, and to a lesser extent of the hippocampus, to total cerebral volume was greater in female than male brains. Although it might be anticipated that the smaller female cerebellum might discriminate between males and females, the differences in the absolute volumes of caudate and white matter, and proportional volumes of caudate and hippocampus, were also sufficiently large to permit classification of gender with 85% accuracy. No other structures within the forebrain were observed to be sexually dimorphic with regard to absolute or proportionate volumes.

Among vertebrate species, morphological dimor-

phism in male and female brains has been explored principally in rodents and avian species, but also in gyrencephalic species including humans and other primates (Goy and McEwen, 1980; Swaab and Hofman, 1984). In humans (LeVay, 1991) and in the pilot fish (Bass, 1992), differential volumes in the rostral hypothalamus and medullary motor nuclei, respectively, have been reported to differentiate males with different sexual or reproductive behavioral patterns. The formal basis of such dimorphism includes differences in neuronal or glial numbers, neuronal somatic or dendritic size, the richness of axonal arborization, and synaptic densities (Gorski, 1984, 1985; Juraska, 1984; Toran-Allerand, 1984).

In rodents, differential volumes or other morphological parameters between males and females have been recognized in the sexually dimorphic nucleus of the preoptic area (SDN-POA) (Gorski, 1984), the hippocampus (Wimer and Wimer, 1985, 1989; Wimer et al., 1988; Jacobs et al., 1990), right–left hemispheric neocortical thickness (Diamond et al., 1983), the visual cortex (Guillamon et al., 1988), the cerebellum, and central nuclei of the amygdaloid complex (Staudt and Dorner, 1976; Guillamon et al., 1988). Striatal dimorphism is cyclic in finches and other song birds (Nottebohm, 1981, 1989). Thus, structures observed here to be volumetrically dimorphic in the young adult human brain are among those observed to be dimorphic in other species. However, in rodents it is observed that these volumetrically dimorphic structures are larger in the male than in the female brain. The principal volumetrically dimorphic structures reported here in the human brain, total cerebellum and cerebral white matter, follow this male larger than female pattern. However, the larger absolute and proportionate volumes of caudate and the larger proportionate volume of the hippocampus in females do not. The larger proportionate volume of the female hippocampus does have a precedent in rodents (Jacobs et al., 1990). The examples of sexual dimorphism that have thus far come to light are in each instance highly individual with respect to animal species or strain and some may be correlated with sexually dimorphic behaviors. Therefore, collectively, examples in nonhuman species should be viewed only cautiously as precedents for sexual dimorphism in human brains.

It has been suggested that structurally dimorphic features of the human brain are associated with a greater dependence of praxic and language functions upon posterior regions in the male but upon frontal regions in the female brain (Kimura, 1992). Male fetal brains have been found to have a significantly greater degree of asymmetry in the striate/extrastriate regions than female brains, and, generally, tended to have cortical volumetric asymmetries favoring the right hemisphere (de Lacoste et al., 1991). In addition, the right hemispheres in the male fetal brains were, on average, 3% larger than the left, while the female hemispheres were either equal in volume or larger on the left. This dimorphism was most notable in specimens younger than 18 weeks of gestation, and although less apparent by observation, was still present after 29 weeks of gestation. The human brain approaches adult size by 4 years of age (Kretschmann et al., 1986a) and the principal "pruning events" of neocortical development appear to have occurred by the end of the first decade of life (Huttenlocher et al., 1982, 1982–1983; Huttenlocher, 1984; Innocenti, 1991; Jernigan et al., 1991; Oppenheim, 1991). If such dimorphic fetal cortical and hemispheric volume asymmetries disappear by adulthood, as implied by the present measures, the underlying developmental mechanisms might be modulated by the complex experiential and hormonal environment operating through puberty, in contrast to that occurring *in utero*.

Experiment has established that sexual hormones are critical determinants of volumetric dimorphisms, and these substances probably have their dimorphic effects though complex combinatorial interactions (Gorski, 1984; Toran-Allerand, 1984). Testosterone acts directly in primate species and indirectly after aromatization to β-estradiol in rodents (Steimer and Hutchison, 1990); estrogenic substances act directly, certainly in rodent species (Dohler et al., 1984; Toran-Allerand, 1984). It has been suggested, for example, by Witelson and associates (Witelson, 1991; Witelson and Nowakowski, 1991) that low levels of testosterone early in development may retard the regressive processes that result in strong lateralization of functions related to handedness, language, and other cognitive functions. α-Fetoprotein is an example of yet another modulating factor that may serve as a critical brake to the neurotrophic or neurotropic histogenetic effects of estrogen in mammalian species including man (Toran-Allerand, 1984). Other determinants, not so confidently ascribed to gonadal (or perhaps adrenal) hormones or specific peptides, may reside more broadly within the male and female genotypes (Gorski, 1984; Toran-Allerand, 1984).

Summary

This database and the methods by which it has been obtained invite a host of additional applications (Cascino et al., 1991; Filipek et al., 1991a; Jack et al., 1992). As an immediate and direct application, the normal values will serve as criteria for recognizing or characterizing the progression of abnormalities of the brain in conditions where the abnormality or the pattern of progression can only be defined by morphometric means (Caviness et al., 1989; Filipek et al., 1991a, 1992). The application of morphometry and analytic tools that provide even finer-grained regional anatomic (Jouandet et al., 1989; Damasio and Frank, 1992; Rademacher et al., 1992) or even architectonic (Damasio et al., 1991) localization, in tandem with rapid imaging methods that offer high spatial–temporal resolution of cognitive events (Belliveau et al., 1991; Kwong et al., 1992), may be expected to support an approach to entirely new sets of hypotheses in cognitive neuroscience.

Notes

This work was supported in part by Grants NS 20489 and NS 24279 (P.A.F., D.N.K.) from the National Institute of Neurological Disorders and Stroke, by HD 27802 (P.A.F , D.N.K.)

from the National Institute of Child Health and Human Development, Bethesda, MD, and by The Oeuvre Alexandre Pascal Fellowship (C.R.) from the Nice-Sophia Antipolis University. D.N.K. also holds a Fairway Trust fellowship. We also express our gratitude to Jack M. Fletcher, Ph.D., for methodological assistance, and to David M. Shera, M S., for statistical advice.

Correspondence should be addressed to Pauline A. Filipek, M D , Center for Morphometric Analysis, Box 61, Neuroscience Center, MGH-East, 149 13th Street, Charlestown, MA 02129.

References

Bass A (1992) Dimorphic male brains and alternative reproductive tactics in a vocalizing fish Trends Neurosci 15:139–145.

Bear D, Schiff D, Saver J, Greenberg M, Freeman R (1986) Quantitative analysis of cerebral asymmetries Fronto-occipital correlation, sexual dimorphism and association with handedness. Arch Neurol 43:598–603.

Belliveau JW, Kennedy DN, McKinstry RC, Buchbinder BR, Weisskoff RM, Cohen MS, Vevea JM, Brady TJ, Rosen BR (1991) Functional mapping of the human visual cortex by magnetic resonance imaging. Science 254:716–719.

Bohm C, Greitz T, Seitz R, Eriksson (1991) Specification and selection of regions of interest (ROIs) in a computerized brain atlas. J Cereb Blood Flow Metab 11:264–268

Breier A, Buchanan RW, Elkashef A, Munson RC, Kirkpatrick B, Gellad F (1992) Brain morphology and schizophrenia: a magnetic resonance imaging study of limbic, prefrontal cortex, and caudate structures Arch Gen Psychiatry 49:921–926.

Cascino GD, Jack CR, Parisi JE, Sharbrough FW, Hirschorn KA, Meyer FB, Marsh WR, O'Brien PL (1991) Magnetic resonance imaging-based volume studies in temporal lobe epilepsy: pathological correlations. Ann Neurol 30:31–36.

Caviness VS, Filipek PA, Kennedy DN (1989) Magnetic resonance technology in human brain science: a blueprint for a program based upon morphometry Brain Dev 1.1–13.

Coffey CE, Wilkinson WE, Parashos IA, Soady SAR, Sullivan RJ, Patterson LJ, Figiel GS, Webb MC, Spritzer CE, Djang WT (1992) Quantitative cerebral anatomy of the aging human brain: a cross-sectional study using magnetic resonance imaging. Neurology 42:527–536

Damasio H, Frank R (1992) Three-dimensional *in vivo* mapping of brain lesions in humans Arch Neurol 49. 137–143.

Damasio H, Kuljis RO, Yuh W, van Hoesen GW, Ehrhardt J (1991) Magnetic resonance imaging of human intracortical structure *in vivo*. Cereb Cortex 1.374–379.

Dekaban AS, Sadowsky D (1978) Changes in brain weights during the span of human life: relation of brain weights to body heights and body weights. Ann Neurol 4:345–356.

de Lacoste MC, Horvath DS, Woodward DJ (1991) Possible sex differences in the developing human fetal brain J Clin Exp Neuropsychol 13.831–846.

DeLisi LE, Hoff AL, Schwartz JE, Shields GW, Halthore SN, Gupta SM, Henn FA, Anand AK (1991) Brain morphology in first-episode schizophrenic-like psychotic patients: a quantitative magnetic resonance imaging study Biol Psychiatry 29:159–175.

DeVito JL, Graham J, Sackett GP (1989) Volumetric growth of the major brain divisions in fetal *Macaca nemestrina* J Hirnforsch 30:479–487.

Diamond MC, Johnson RE, Young D, Singh SS (1983) Age-related morphological differences in the rat cerebral cortex and hippocampus. male-female, right-left. Exp Neurol 81:1–13.

Dohler KD, Hancke JL, Srivastava SS, Hofmann C, Shryne JE, Gorski RA (1984) Participation of estrogens in female sexual differentiation of the brain; neuroanatomical, neuroendocrine and behavioral evidence. Prog Brain Res 61. 99–117.

Escalona PR, McDonald WM, Doraiswamy PM, Boyko OB, Husain MM, Figiel GS, Laskowitz D, Ellinwood EH, Krishnan KRR (1991) *In vivo* stereological assessment of human cerebellar volume: effects of gender and age. Am J Neuroradiol 12:927–929.

Falk D, Hildebolt C, Cheverud J, Kohn LA, Figiel G, Vannier M (1991) Human cortical asymmetries determined with 3D MR technology. J Neuromethods 39:185–191

Filipek PA, Kennedy DN, Caviness VS, Rossnick SL, Spraggins TA, Starewicz PM (1989) MRI-based brain morphometry: development and application to normal controls. Ann Neurol 25:61–67

Filipek PA, Kennedy DN, Rademacher J, Caviness VS (1990) Error and variability incurred with MRI-based morphometry. Ann Neurol 28:459.

Filipek PA, Kennedy DN, Caviness VS (1991a) Volumetric analyses of central nervous system neoplasm based on MRI. Pediatr Neurol 7:347–351.

Filipek PA, Kennedy DN, Pitcher DA, Caviness VS (1991b) MRI-based morphometric analysis. reproducibility across multiple systems and pulse sequences over time on a single volunteer. Proc Soc Mag Res Med 10:753.

Filipek PA, Kennedy DN, Caviness VS (1992) Neuroimaging in child neuropsychology. In. Handbook of neuropsychology (Boller F, Grafman J, eds), Vol 6, Child neuropsychology (Rapin I, Segalowitz S, eds), pp 301–329. Amsterdam: Elsevier.

Galaburda AM, Sanides F, Geschwind N (1978) Cytoarchitectonic left-right asymmetries in the temporal speech region. Arch Neurol 35:812–817.

Galaburda AM, Corsiglia J, Rosen GD, Sherman GF (1987) Planum temporale asymmetry: reappraisal since Geschwind and Levitsky. Neuropsychologia 25:853–868.

Geschwind N, Levitsky W (1968) Human brain: left-right asymmetries in temporal speech region. Science 161:186–187.

Gorski RA (1984) Critical role for the medial preoptic area in the sexual differentiation of the brain. Prog Brain Res 61:129–145.

Gorski RA (1985) Sexual dimorphisms of the brain. J Anim Sci 61[Suppl 3]:38–61.

Gould SJ (1981) The mismeasure of man. New York: Norton.

Goy RW, McEwen BS (1980) Sexual differentiation of the brain, pp 1–233. Cambridge, MA: MIT Press

Greitz T, Bohm C, Holte S, Eriksson L (1991) A computerized brain atlas: construction, anatomical content and some applications J Comput Assist Tomogr 15:26–38

Guillamon A, Segovia S, del Abril A (1988) Early effects of gonadal steroids on the neuron number in the medial posterior region and the lateral division of the bed nucleus of the stria terminalis in the rat. Dev Brain Res 44. 281–290.

Harper C, Mina L (1981) A comparison of Australian Caucasian and aboriginal brain weights Clin Exp Neurol 18: 44–51

Harris GJ, Pearlson GD, Peyser CE, Aylward EH, Roberts J, Barta PE, Chase GA, Folstein SE (1992) Putamen volume reduction on magnetic resonance imaging exceeds caudate changes in mild Huntington's disease. Ann Neurol 31:69–75.

Hatazawa J, Ito M, Yamamura H, Matsuzawa T (1982) Sex difference in brain atrophy during aging: a quantitative study with computed tomography J Am Geriatr Soc 30: 235–239.

Hollingshead AB (1975) Four factor index of social status. Unpublished manuscript, Yale University Department of Sociology.

Holloway RL (1980) Within species brain-body weight variability. Am J Physiol Anthropol 53:109–121.

Hubbard B, Anderson J (1981) A quantitative study of cerebral atrophy in old age and senile dementia. J Neurol Sci 50:135–145.

Huttenlocher PR (1984) Synapse elimination and plasticity in developing human cerebral cortex. Am J Ment Defic 88:488–496.

Huttenlocher PR, DeCourten C, Garey LJ, Van der Loos H (1982) Synaptogenesis in human visual cortex—evidence for synapse elimination during normal development. Neurosci Lett 33:247–252

Huttenlocher PR, DeCourten C, Garey LJ, Van der Loos H (1982–1983) Synaptic development in human cerebral cortex. Int J Neurol 16–17:144–154.

Innocenti GM (1991) The development of projections from cerebral cortex. Prog Sensory Physiol 12:65–114.

Jack CR, Gehring DG, Sharbrough FW, Felmlee JP, Forbes G, Hench VS, Zinsmeister AR (1988) Temporal lobe volume measurements from MR images: accuracy and left-right asymmetry in normal persons. J Comp Assist Tomogr 12.21–29.

Jack CR, Twomey CK, Zinsmeister AR, Sharbrough FW, Petersen RC, Cascino GD (1989) Anterior temporal lobes and hippocampal formations: normative volumetric measurements from MR images in young adults. Radiology 172:549–554.

Jack CR, Bentley MD, Twomey CK, Zinsmeister AR (1990) MR imaging-based volume measurements of the hippocampal formation and anterior temporal lobe: validation studies Radiology 176:205–209.

Jack CR, Sharbrough FW, Cascino GD, Hirschorn KA, O'Brien PC, Marsh WR (1992) Magnetic resonance image-based hippocampal volumetry: correlation with outcome after temporal lobectomy. Ann Neurol 31.202–211.

Jacobs LF, Gaulin SJ, Sherry DF, Hoffman GE (1990) Evolution of spatial cognition: sex-specific patterns of spatial behavior predict hippocampal size. Proc Natl Acad Sci USA 87:6349–6352.

Jerison HJ (1973) Gross brain indices and the meaning of brain size. In. Evolution of the brain and intelligence, pp 55–81 New York. Academic

Jernigan TL, Tallal PA (1990) Late childhood changes in brain morphology observable with MRI Dev Med Child Neurol 32:379–385.

Jernigan TL, Trauner DA, Hesselink JR, Tallal PA (1991) Maturation of human cerebrum observed *in vivo* during adolescence. Brain 114:2037–2049.

Jouandet ML, Tramo MJ, Herron MJ, Hermann A, Loftus WC, Bazell J, Gazzaniga MS (1989) Brainprints: computer-generated two-dimensional maps of the human cerebral cortex *in vivo* J Cognit Neurosci 1.88–117.

Juraska JM (1984) Sex differences in developmental plasticity in the visual cortex and hippocampal dentate gyrus Prog Brain Res 61:205–214.

Kennedy DN (1986) A system for three-dimensional analysis of magnetic resonance images. MS thesis, Department of Nuclear Engineering, Massachusetts Institute of Technology

Kennedy DN, Nelson AC (1987) Three-dimensional display from cross-sectional tomographic images: an application to magnetic resonance imaging. IEEE Trans Med Imaging 6:134–140.

Kennedy DN, Filipek PA, Caviness VS (1989) Anatomic segmentation and volumetric calculations in nuclear magnetic resonance imaging. IEEE Trans Med Imaging 8 1–7.

Kennedy DN, Rademacher J, Filipek PA, Caviness VS (1991) Three-dimensional anatomical cross-referencing in magnetic resonance imaging. Proc Soc Mag Res Med 10:754.

Kertesz A, Polk M, Black SE, Howell J (1990) Sex, handedness, and the morphometry of cerebral asymmetries on magnetic resonance imaging. Brain Res 15:40–48.

Kimura D (1992) Sexual differences in the brain. Sci Am 267:118–125

Klekamp J, Riedel A, Harper C, Kretschmann H-J (1987) A quantitative study of Australian aboriginal and Caucasian brains. J Anat 150:191–210.

Kretschmann H-J, Schleicher A, Wingert F, Zilles K, Loblich JH (1979) Human brain growth in the 19th and 20th century J Neurol Sci 40:169–188.

Kretschmann H-J, Kammradt G, Krauthausen I, Sauer B, Wingert F (1986a) Brain growth in man. Bibl Anat 28:1–26

Kretschmann H-J, Kammradt G, Krauthausen I, Sauer B, Wingert F (1986b) Growth of the hippocampal formation in man. Bibl Anat 28:27–52.

Kwong KK, Belliveau JW, Chesler DA, Goldberg IE, Weisskoff RM, Poncelet BP, Kennedy DN, Hopel BE, Cohen MS, Turner R, Cheng H-M, Brady TJ, Rosen BR (1992) Dynamic magnetic resonance imaging of human brain activity during primary sensory stimulation. Proc Natl Acad Sci USA 89:5675–5679.

LeMay M, Kido DK (1978) Asymmetries of the cerebral hemispheres on computed tomograms. J Comp Assist Tomogr 2:471–476.

LeVay S (1991) A difference in hypothalamic structure between heterosexual and homosexual men Science 253:1034–1037

Maxwell WE, Delaney HD (1990) Designing experiments and analyzing data: a model comparisons approach. Belmont, CA Wadsworth

Miller AKH, Alston RL, Corsellis JAN (1980) Variation with age in the volumes of grey and white matter in the cerebral hemispheres of man. measurements with an image analyzer. Neuropathol Appl Neurobiol 6.119–132.

Nottebohm F (1981) A brain for all seasons: cyclical anatomical changes in song control nuclei of the canary brain. Science 214:1368–1370.

Nottebohm F (1989) From bird song to neurogenesis. Sci Am 260.74–79.

Oldfield R (1971) The assessment and analysis of handedness Neuropsychologia 9:97–113.

Ono M, Jubik S, Abernathy CD (1990) Atlas of the cerebral sulci, pp 1–218 New York: Thieme.

Oppenheim RW (1991) Cell death during development of the nervous system. Annu Rev Neurosci 14.453–501

Pakkenberg B (1988) Post-mortem study of chronic schizophrenic brains Br J Psychol 151.744–752

Paul F (1971) Biometrische Analyse der Frischvolumina des Grosshirnrinde und des Prosencephalon von 31 menschlichen, adulten Gehirnen. Z Anat Entwicklungsgesch 133:325–368

Rademacher J, Galaburda AM, Kennedy DN, Filipek PA, Caviness VS (1992) Human cerebral cortex: localization, parcellation, and morphometry with magnetic resonance imaging J Cognit Neurosci 4:352–374.

Rademacher J, Caviness VS, Steinmetz H, Galaburda AM (1993) Topographical variation of the human primary cortices: implications for neuroimaging, brain mapping and neurobiology. Cereb Cortex 3.313–329.

Risse GL, Gates J, Lund G, Maxwell R, Rubens AB (1989) Interhemispheric transfer in patients with incomplete section of the corpus callosum. Anatomic verification with magnetic resonance imaging Arch Neurol 46:437–443

Schwartz M, Creasey H, Grady CL, DeLeo JM, Frederickson HA, Cutler NR, Rapoport SI (1985) Computed tomographic analysis of brain morphometrics in 30 healthy men, aged 21 to 81 years. Ann Neurol 17:146–157.

Shenton ME, Kikinis R, Jolesz FA, Pollak SD, LeMay M, Wible CG, Hokama H, Martin J, Metcalf D, Coleman M, McCarley RW (1992) Abnormalities of the left temporal lobe and thought disorder in schizophrenia: a quantitative magnetic resonance imaging study. N Engl J Med 327:604–612.

Staudt J, Dorner G (1976) Structural changes in the medial and central amygdala of the male rat, following castration and androgen treatment. Endokrinologie 67:296–300.

Steimer T, Hutchison JB (1990) Is androgen-dependent aromatase activity sexually differentiated in the rat and dove preoptic area? J Neurobiol 21:787–795

Steinmetz H, Rademacher J, Huang YX, Hefter H, Zilles K, Thron A, Freund JH (1989) Cerebral asymmetry: MR planimetry of the human planum temporale. J Comput Assist Tomogr 13:996–1005.

Steinmetz H, Rademacher J, Jancke L, Huang H, Thron A, Zilles K (1990) Total surface of temporo-parietal intrasylvian cortex: diverging left-right asymmetries. Brain Lang 39:357–372.
Steinmetz H, Jancke L, Kleinschmidt A, Schlaug G, Volkmann J, Huang Y (1992) Sex but no hand difference in the isthmus of the corpus callosum Neurology 42:749–752.
Swaab DF, Hofman MA (1984) Sexual differentiation of the human brain: a historical perspective Prog Brain Res 61. 361–373
Talairach J, Tournoux P (1988) Co-planar stereotaxic atlas of the human brain. New York. Thieme.
Toran-Allerand CD (1984) On the genesis of sexual differentiation of the central nervous system: morphogenetic consequences of steroidal exposure and possible role of alpha-fetoprotein. Prog Brain Res 61:63–97
Watson C, Andermann F, Gloor P, Jones-Gotman M, Peters T, Evans A, Olivier A, Melanson D, Leroux G (1992) Anatomic basis of amygdaloid and hippocampal volume measurement by magnetic resonance imaging. Neurology 42:1743–1750.
Wessely W (1970) Biometrische Analyse der Frischvolumina des Rhombencephalon, des Cerebellum und der Ventrikel von 31 adulten menschlichen Gehirnen. J Hirnforsch 12:11–28.
Wimer CC, Wimer RE (1989) On the sources of strain and sex differences in granule cell number in the dentate area of house mice. Dev Brain Res 48:167–176.
Wimer RE, Wimer CC (1985) Three sex dimorphisms in the granule cell layer of the hippocampus in house mouse. Brain Res 328:105–109.
Wimer RE, Wimer CC, Alameddine L (1988) On the development of strain and sex differences in granule cell number in the area dentata of house mice. Brain Res 470: 191–197.
Witelson SF (1989) Hand and sex differences in the isthmus and genu of the corpus callosum: a postmortem morphological study Brain 112:799–835
Witelson SF (1991) Neural sexual mosaicism: sexual differentiation of the human temporo-parietal region for functional asymmetry. Psychoneuroendocrinology 16: 131–153.
Witelson SF, Kigar DL (1992) Sylvian fissure morphology and asymmetry in men and women. bilateral differences in relation to handedness in men J Comp Neurol 323: 326–340.
Witelson SF, Nowakowski RS (1991) Left out axons make men right. a hypothesis for the origin of handedness and functional asymmetry Neuropsychologia 29:327–333.
Zatz LM, Jernigan TL, Ahumada AJ (1982) Changes on computed cranial tomography with aging: intracranial fluid volume Am J Neuroradiol 3:1–11.
Zilles K, Armstrong E, Schleicher A, Kretschmann H-J (1988) The human pattern of gyrification in the cerebral cortex Anat Embryol (Berl) 179:173–179.